Inductively coupled plasma etching of SiC in SF6/O-2 and etch-induced surface chemical bonding modifications

Inductively coupled plasma etching of SiC in SF6/O2 and etch-induced surface chemical bonding modifications

Liudi Jiang, R. Cheung, R. Brown, and A. Mount

Citation: J. Appl. Phys. **93**, 1376 (2003); doi: 10.1063/1.1534908
View online: http://dx.doi.org/10.1063/1.1534908
View Table of Contents: http://jap.aip.org/resource/1/JAPIAU/v93/i3
Published by the AIP Publishing LLC.

Inductively coupled plasma etching of SiC in SF_6/O_2 and etch-induced surface chemical bonding modifications

Liudi Jiang[a] and R. Cheung
School of Engineering and Electronics, Scottish Microelectronics Centre, The University of Edinburgh, King's Buildings, West Mains Road, Edinburgh EH9 3JF, United Kingdom

R. Brown and A. Mount
Department of Chemistry, Joseph Black Building, The University of Edinburgh, West Mains Road, Edinburgh EH9 3JJ, United Kingdom

(Received 5 August 2002; accepted 12 November 2002)

4H silicon carbide (SiC) substrates were dry etched in an inductively coupled plasma (ICP) system, using SF_6/O_2 gas mixtures. Etch rate and etch mechanisms have been investigated as a function of oxygen concentration in the gas mixture, ICP chuck power, work pressure, and flow rate. Corresponding to these etch conditions, surface information of the etched SiC has been obtained by x-ray photoelectron spectroscopy measurements. The fact that no obvious Si–Si and Si–F bonds were detected on the etched surface of SiC in all our etch experiments suggests efficient removal of Si atoms as volatile products during the processes. However, various kinds of C–F bonds have been detected on the etched SiC surface and the relative intensities of these bonds vary with the etch conditions. In addition, the nature of the incorporated F atoms on the etched surface also depends strongly on etch conditions, which was identified by the change of the relative ratio between semi-ionic and covalent carbon fluorine bonds. The electrical behavior for different bond structures on the etched SiC surface can be one of the basic reasons affecting related devices. © *2003 American Institute of Physics.* [DOI: 10.1063/1.1534908]

I. INTRODUCTION

Silicon carbide (SiC) has attracted considerable interest as a very promising generation semiconductor material for high-temperature, high-power, and high-frequency electronic device applications,[1] due to its unique properties such as large band gap (2.3–3.3 eV), large breakdown field (2.5×10^6 V/cm), excellent thermal conductivity [4.9 W/ (cm K)], and saturated electron drift velocity (2×10^7 cm/s), etc. Because of its great hardness, high-wear resistivity, excellent thermal conductivity, and chemical inertness, SiC also becomes an excellent candidate for microsensor and microactuator applications in microelectromechanical systems (MEMS), especially in harsh environments. Due to the large bond energies between Si and C and therefore great chemical inertness, plasma-based dry etching is required as the only practical way[2] to deep etch SiC for the fabrication of MEMS. In most of the dry etch techniques applied so far, inductively coupled plasma (ICP) becomes a very promising technique because of high flux with lower-ion energy, which enables the achievement of excellent anisotropy etch at a high-etch rate for SiC even at relatively low-bias voltages.[3,4] Although SiC etch rates in an ICP system have been investigated, there is still a lack of understanding of the etch mechanisms.

It is known that surface damage and contamination induced during dry etch patterning of semiconductors can significantly affect the properties of the material, subsequent processing, and device performance.[5,6] Therefore, in order to obtain better understanding, prediction, and even control of the properties and behavior of the fabricated devices, it is essential to characterize and investigate the surface microstructure modifications caused by dry etch processes. Although surface morphology of etched SiC has been studied,[7–9] there is lack of investigation on the etch products on the surface of the etched SiC, especially the variation of these etch products under different etch conditions. Furthermore, the study on the surface chemistry of the etched SiC can also contribute to a better understanding of etch mechanisms of SiC.

In this article, we report on our work on the etching results of SiC using ICP in SF_6/O_2 gas mixtures. Since the surface microstructure of etched SiC is closely related to the etch mechanisms, by analyzing the corresponding etch-induced surface chemical bonding modifications from SiC samples etched at different conditions, light has been shed upon the etch mechanisms as well as the final conditions of the etched SiC surfaces.

II. EXPERIMENT

The samples used were bulk 4H–SiC substrates from Cree, Inc. which were *n*-type (N doped) with carrier density of $\sim10^{16}\,\mathrm{cm}^{-3}$. A silicon dioxide ($SiO_2$) layer of $\sim6\,\mu$m thick was firstly deposited on the cleaned SiC substrates using a plasma-enhanced chemical-vapor deposition system and then the samples were masked with photolithography patterned photoresist (Megaposit SPR2-2FX 1.3). A plasmatherm PK2440 reactive ion etching system was then used to etch the photoresist patterned SiO_2 layer to expose the SiC substrate. The remaining photoresist was then removed by

[a]Electronic mail: liudi.jiang@ee.ed.ac.uk

acetone and isopropanol afterwards. The SiO_2 patterned SiC samples were etched in a Surface Technology Systems (STS) multiplex ICP system for 10 min at ICP coil power 1 kW. A water cooling system has been applied to keep the chunk at room temperature during etch processes. The other etch conditions have been varied as stated separately. A Dektak model 8000 surface profiler was used to measure the etch depth after the oxide mask had been removed using hydrofluoric acid, rinsed by deionized water, and blown dry with N_2 gas.

Etched SiC samples were loaded in a ultrahigh vacuum (UHV) x-ray photoelectron spectroscopy (XPS) chamber as soon as possible after the removal of oxide mask. All the XPS analyses were performed on the etched SiC surface using a monochromatic Al $K\alpha$ ($h\nu = 1486.6$ eV) x-ray source operating at 15 kV. The base pressure of the XPS chamber was $\sim 2.9\times 10^{-9}$ mbar and then increased to $\sim 3\times 10^{-8}$ mbar by letting in a small amount of argon gas and then slightly deionized in order to prevent a possible charge effect during the measurements. All the samples were mounted on a metal stage using adhesive conductive carbon tapes in order to provide a conductive connection between the samples and the stage.

During the analysis of the XPS results, it was found that, because our doped SiC samples have very low resistivity ($\sim 0.3\,\Omega$ cm) and also with the assistance of the deionized Ar^+ ions in the chamber, there was only very small charge effect observed. It was reported[10] that the energy separation between C 1*s* and Si 2*p* core levels in SiC depends only on their chemical shifts and is independent of the Fermi-level position at the surface. By analysing all our XPS results, it was found that

$$\Delta E = E(\mathrm{C1}s) - E(\mathrm{Si2}p) = 182.3 \pm 0.2\ \mathrm{eV}$$

$E(\mathrm{C1}s)$ and $E(\mathrm{Si2}p)$ are the peak positions of C 1*s* and Si 2*p* core-level spectra. This agrees with the measured value for SiC crystals.[10] Also, all the peak positions of C 1*s* spectra are at 282.5 ± 0.3 eV which is considered further proof that C 1*s* spectra are dominated by the C component from SiC. Therefore, we have aligned all the C 1*s* spectra with the highest-peak position at 282.5 eV and other peaks have been moved accordingly. The resulted binding energy of Si 2*p* for all the samples is at 100.2 ± 0.1 eV, which is a typical fingerprint for the Si–C bond.[11–13] All the XPS core-level spectra have been analyzed by deconvolution after subtraction of the background from the spectra by the linear mode and have been fitted by Gaussian peaks.

III. RESULTS AND DISCUSSION

A. Typical surface chemistry induced by etch process

XPS measurements have been carried out on the original unetched 4H–SiC substrates. Figures 1(a) and 1(b) show the core-level spectra of both C 1*s* and Si 2*p* photoelectron peaks of the original SiC substrate, respectively. The deconvoluted Gaussian peaks are also shown in Fig. 1. The component peak positioned at ~ 282.6 eV is ascribed to C–Si bonds. The other two component peaks at ~ 284.5 and ~ 285.3 eV are attributed to adventitious carbon and unsaturated carbon

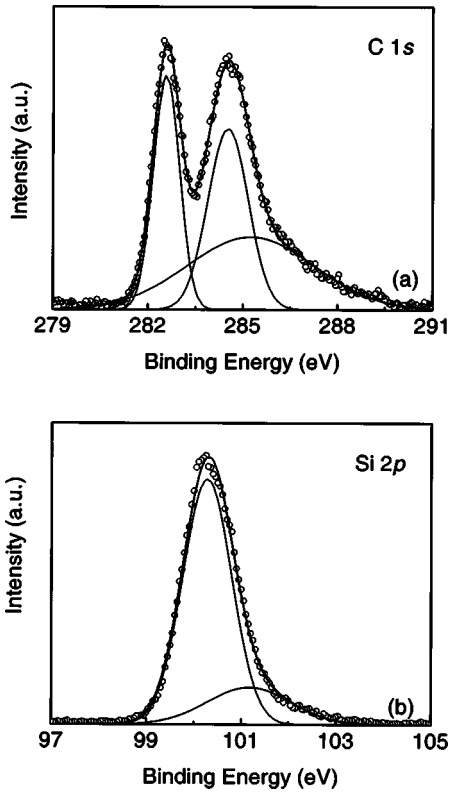

FIG. 1. (a) C 1*s* and (b) Si 2*p* photoelectron spectra of original 4H–SiC surface.

with only H or C neighbors[14] originating from contamination because the substrates have been exposed in air. The Si 2*p* peak is slightly asymmetric and can be decomposed into two Gaussian peaks. The dominant component peak at ~ 100.3 eV is a fingerprint of the C–Si bond and the component peak located at ~ 101.2 eV suggests the existence of O–Si–C bond.[11,15]

Typical photoelectron spectra of an etched SiC sample with Gaussian distribution fits to component peaks are shown in Fig. 2. The C 1*s* peak is decomposed into six Gaussian peaks. The main component at ~ 282.5 eV is from C–Si bonds existing in the crystalline substrate. SiC can be amorphized since the charge transfer from C to Si characterized by the Phillips ionicity $f_i = 0.18$ is low enough.[16,17] Also, it is reported[18] that a physical sputtering effect leads to the formation of a thin amorphous layer on the surface of etched SiC. Therefore, in Fig. 2(a), we attribute the C 1*s* component at ~ 283.7 eV to the amorphous C–Si (*a*-SiC) form which was caused by inevitable physical sputtering during the etch processes. The similar behavior can be supported by the results of Smith and Black[11] where a shift of the C 1*s* binding energy (BE) of crystalline SiC was observed after sputtering. Also a decrease of C 1*s* BE from ~ 283.4 to ~ 282.6 eV during the crystallization of SiC material was reported.[12,19] Furthermore, as the most electronegative element, F radicals in the etching plasma can react with C atoms from the bond breaking in SiC and have a marked effect on the C 1*s* core-level BE, namely, leads C 1*s* peaks towards high BE.[20] As shown in Fig. 2(a), the C 1*s* component at ~ 287.8, ~ 289.8, and ~ 292.4 eV are identified with C at-

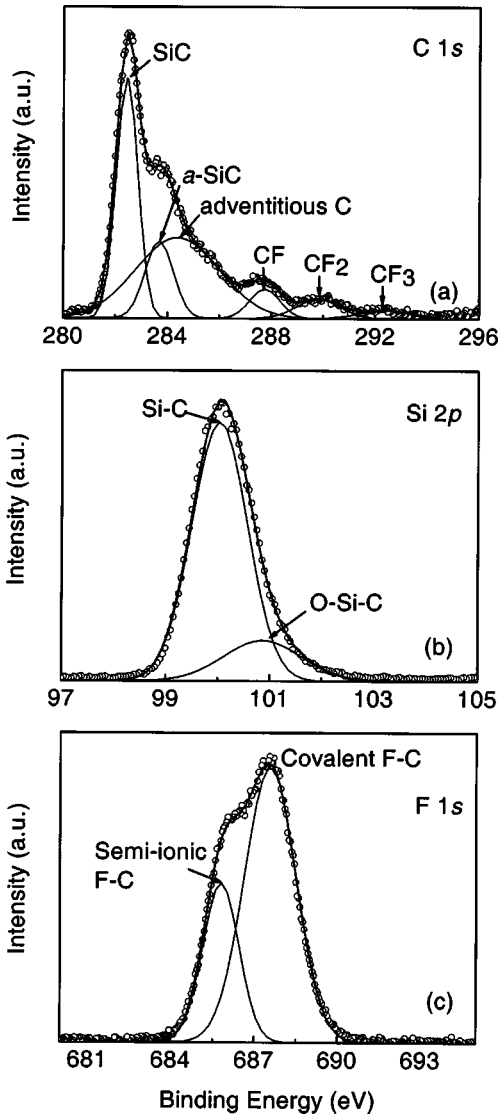

FIG. 2. Typical (a) C 1*s*, (b) Si 2*p*, and (c) F 1*s* photoelectron spectra of an etched SiC surface. (Chuck power=120 W, DC bias=510 V, SF_6 flow rate =60 sccm, O_2 flow rate=6.6 sccm, and pressure=5 mT).

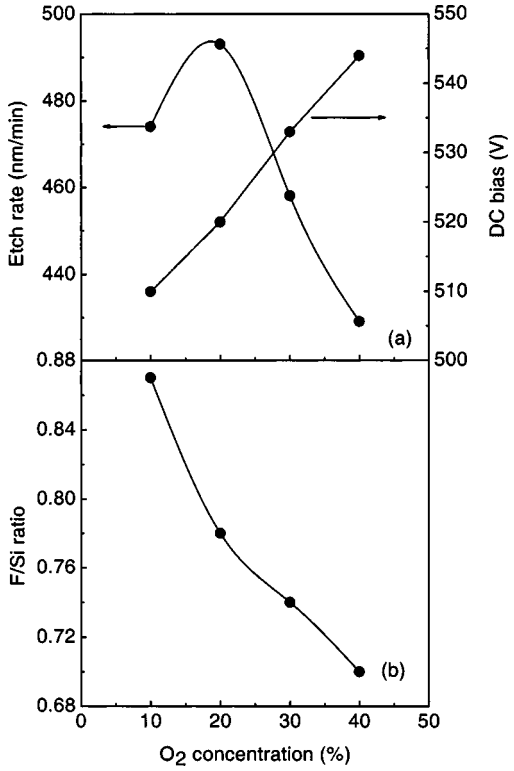

FIG. 3. (a) Etch rate and DC bias (b) F/Si ratio vs O_2 concentration in SF_6/O_2 gas mixture. (Chuck power=120 W, SF_6 flow rate=60 sccm, and pressure=5 mT).

oms bonded to one (CF), two (CF_2), and three (CF_3) F atoms, respectively.[20–23]

Comparing Figs. 2(b) and 1(b), we found that the etch process did not affect very much either the shape or the energy positions of Si 2*p* spectra. The absence of the Si 2*p* component at ~99 eV (Ref. 15) and the very weak broad feature at higher energy (101–104) eV (Ref. 24) indicate that there is little Si–Si and Si–F bonds on the etched surface, respectively. This means that, during the etch process, most of the Si atoms from the bond breaking in the SiC have been efficiently removed by formation of volatile products such as SiF_x. [25,26] Because Si 2*p* spectra from all the etched SiC surface are very similar and seem to be independent of the etch conditions, they will not be presented in the following sections.

Fluorine photoelectron spectrum has been detected in the etched SiC sample, as shown in Fig. 2(c). Bond breaking of SiC during etching processes can induce sp^2 hybridized amorphous C atoms and their π electron systems. F radicals in the plasma can react with these sp^2 bonded C atoms and play a role of electron acceptors in C–F bonds, involving the corresponding π electron system from the C atoms. It is known that,[20] there are ionic, semi-ionic, and covalent C–F bonds. In ionic-type intercalation C–F bonds, these π electrons are strongly delocalized. The BE of intercalated F anion varies from ~683 to ~685 eV.[27,28] With the increase of the F density, F atoms get closer to the C atoms. The localization of the π electrons of the C atoms concerned increase and the ionic character of C–F bonds decrease. Therefore, semi-ionic-type C–F bond forms and corresponding BE of F 1*s* is from ~685.7 to ~686.6 eV. [27,28] When the degree of localization of the π electrons of the C atoms concerned increases strongly, semi-ionic C–F bond become a covalent bond.[29] The F 1*s* level is between ~687.4 and ~687.8 eV.[28] By deconvoluting the F 1*s* spectra as shown in Fig. 2(c), we found that both semi-ionic (~685.8 eV) and covalent (~687.56 eV) C–F bonds exist on the etched SiC surface. The conductivity of fluorocarbon compounds is very much related to the bonding nature between F and C with the covalent bond leading to a higher resistivity comparing with semi-ionic and ionic bonds,[20] the existence of different C–F bonds can be one of the basic reasons affecting the properties of related devices such as Schottky diodes.

In the following investigations, SiC substrates have been etched at various etch conditions. Both etch mechanism and the corresponding surface chemical bonding modifications are investigated.

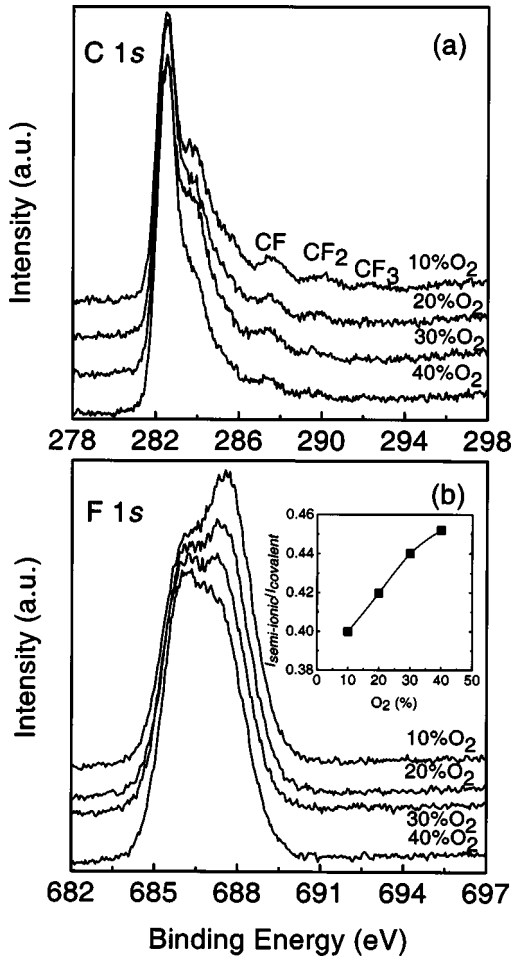

FIG. 4. (a) C 1*s* and (b) F 1*s* photoelectron spectra of SiC surface etched at different O_2 concentration in SF_6/O_2 gas mixture. The inset shows $I_{\text{semi-ionic}}/I_{\text{covalent}}$ ratio in the F 1*s* spectra as a function of O_2 concentration.

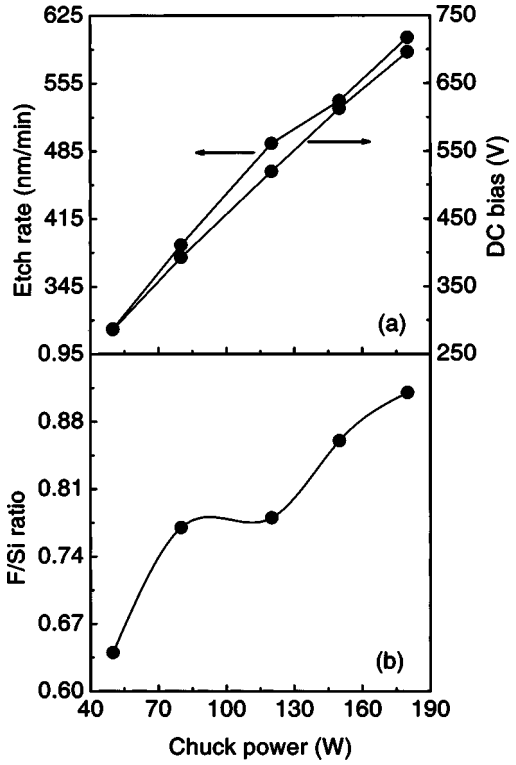

FIG. 5. (a) Etch rate and DC bias and (b) F/Si ratio vs applied chuck power. (SF_6 flow rate = 60 sccm, O_2 flow rate = 15 sccm, and pressure = 5 mT).

B. Influence of oxygen concentration in gas mixtures

Figure 3(a) shows both etch rate and resulted dc bias as a function of O_2 concentration in gas mixtures. It was found that the peak etch rate is at 20% O_2. Although the O_2 addition to SF_6 plasma provides another pathway for volatilizing C in the forms of CO, CO_2 (Refs. 30,31), etc., which increases the etch rate, it also produces SiO_2 on the surface which can prevent the etch process.[26] Therefore, an optimum concentration of 20% O_2 in a SF_6/O_2 gas mixture was obtained due to this competition, as shown in Fig. 3(a). This result agrees with previous publications.[26]

The surface chemical compositions have been calculated according to the XPS results. The sensitivity factors used for C, Si, O, and F are 0.25, 0.27, 0.66, and 1, respectively.[32] The relative ratio of F/Si versus O_2 concentration is shown in Fig. 3(b). The relative concentration of F decreases with the increase of O_2 in the gas mixture. When there is more O_2 in the plasma, more C atoms were removed by volatile products like CO, CO_2, etc. This leads to less concentration of C–F groups which is proved in Fig. 4(a), where the intensity of the C 1*s* component from CF, CF_2, and CF_3 groups becomes weaker with the increase of O_2 concentration. The decrease of the F relative content in Fig. 3(b) can be explained by the decrease of the C–F bonds with the increase of O_2 in the gas mixtures.

Figure 4(b) shows the F 1*s* spectra from the SiC etched at different O_2 concentrations. It is noticed that with the increase of O_2%, the dominant F 1*s* is changed gradually from covalent to semi-ionic C–F bonds. After subtraction of the background by the linear mode, all the F 1*s* spectra can be fitted into two Gaussian component peaks which correspond to semi-ionic (~685.8 eV) and covalent (~687.5 eV) C–F bonds, respectively. By using the area intensity of the semi-ionic ($I_{\text{semi-ionic}}$) and covalent (I_{covalent}) component peaks, the relative intensity ratio ($I_{\text{semi-ionic}}/I_{\text{covalent}}$) versus O_2% has been calculated and is shown in the inset of Fig. 4(b). This result can be explained by Fig. 3(b), where the relative F concentration decreases with addition of O_2.

Because a maximum SiC etch rate was found at 20% O_2, in the following etch experiments, all the SiC were etched at conditions with 20% O_2 in SF_6/O_2 gas mixtures.

C. Influence of chuck power

As shown in Fig. 5(a), in our ICP system, the resulted dc bias increases with applied chuck power. The higher-dc bias causes more efficient bond breaking in SiC and drives surface chemical reaction more rapidly.[26] Therefore, higher-etch rates were achieved at higher-chuck powers.

F/Si relative ratio is calculated and shown in Fig. 5(b) as a function of chuck power. With the increase of chuck power, namely, with the increase of the dc bias, relatively more incorporated F is observed. Because higher-energy ion bombardment caused by higher-DC voltages during dry etching

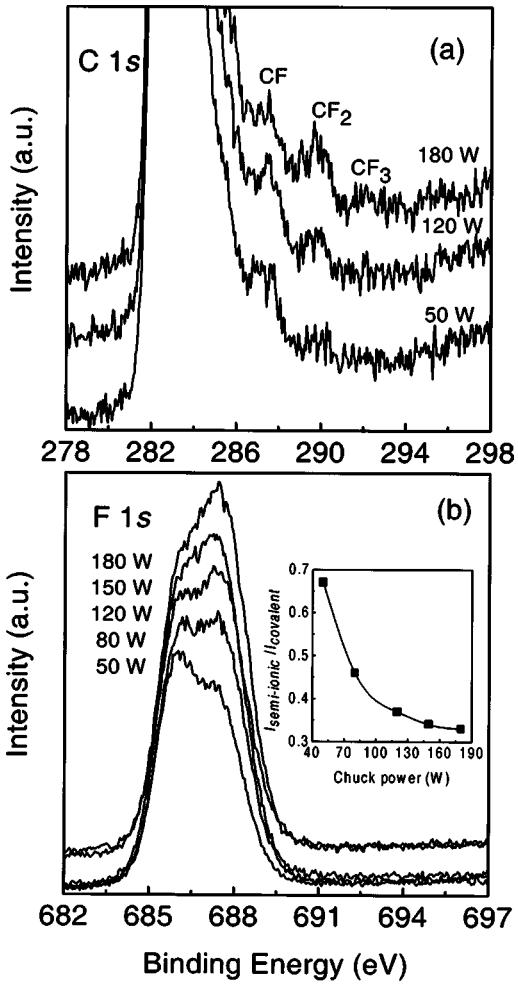

FIG. 6. (a) C 1*s* and (b) F 1*s* photoelectron spectra of SiC surface etched at different chuck powers. The inset shows $I_{\text{semi-ionic}}/I_{\text{covalent}}$ ratio in the F 1*s* spectra as a function of chuck power.

of SiC enhances the cross-linked bonds between F and C,[22] Fig. 6(a) shows that the intensities of C–F bonds increase with the applied chuck powers. This can be seen more clearly from the intensity change of the CF_2 bond. Also, the CF_3 bond is only observed in the sample etched at 180 W chuck power, while it is not obvious in the other two samples etched at lower-chuck powers. This indicates that, with the increase of the incorporated F concentration, the formation of C–F bonds is in the order of CF, CF_2, and CF_3, which is in agreement with the results from Ronning *et al.*,[21] where the growth of fluorinated carbon films was studied.

F 1*s* spectra in Fig. 6(b) show clearly the decrease of semi-ionic to covalent C–F bonds with an increase of the applied chuck power and etch rate, corresponding to the increase of the concentration of the incorporated F, as shown in Fig. 5(b). The same method as described in Sec. III B has been used to calculate the relative intensity ratio ($I_{\text{semi-ionic}}/I_{\text{covalent}}$) and the result is shown in the inset of Fig. 6(b). Based on the difference in the electronic behavior between semi-ionic and covalent C–F bonds,[20] the above observation suggests that, at higher etch rate, the etched SiC surface becomes less conductive.

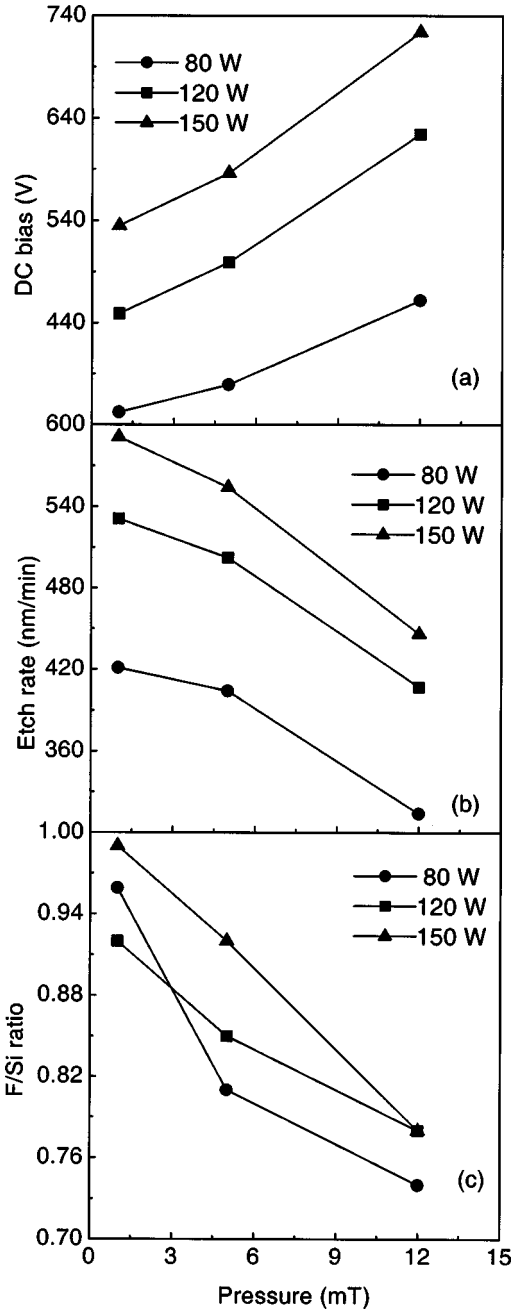

FIG. 7. (a) DC bias, (b) etch rate, (c) F/Si ratio vs pressure at chuck power of 80, 120, and 150 W, respectively. (SF_6 flow rate=40 sccm and O_2 flow rate=10 sccm).

D. Influence of work pressure

The effects of work pressure are also investigated. The chuck powers were kept constant during our pressure experiments. Under the pressure regime investigated in our experiments, because the mean free path and average lifetime of ions are reduced at higher pressure, the ion content decreases with the increase of working pressure which resulted in higher-dc bias, as shown in Fig. 7(a). Furthermore, at high pressures, the mean free path of ions can be reduced to be much shorter than the length of the sheath in the plasma. This effect can reduce the directionality of the ions impinging on the SiC samples, thereby reducing the etch rates at higher-work pressures, as shown in Fig. 7(b).

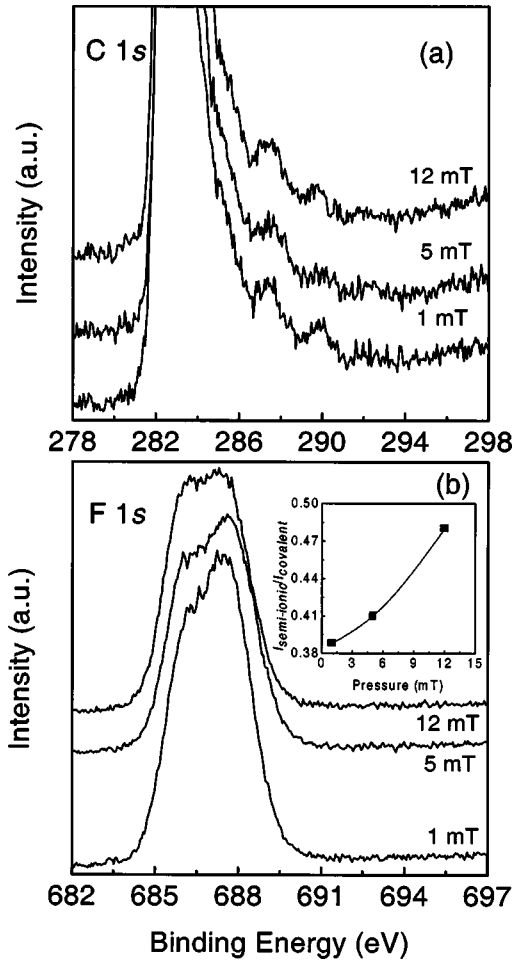

FIG. 8. (a) C 1*s* and (b) F 1*s* photoelectron spectra of SiC surface etched at different pressure. (Chuck power=120 W, SF_6 flow rate=40 sccm, and O_2 flow rate=10 sccm).

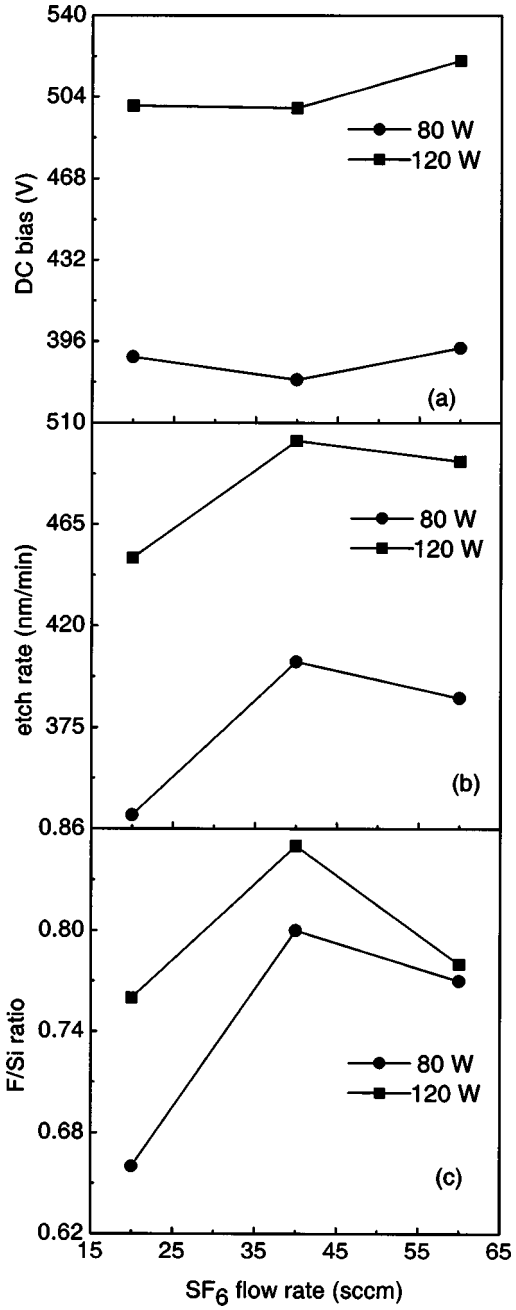

FIG. 9. (a) DC bias, (b) etch rate, and (c) F/Si ratio vs SF_6 flow rate at chuck power of 80 and 120 W, respectively. Note that 5, 10, and 15 sccm O_2 were used with 20, 40, and 60 sccm SF_6 in the SF_6/O_2 gas mixtures during etch. (Pressure=5 mT).

Figure 7(c) shows that the relative content of F also decreases with the pressure. This is because the lower-reactive ion energies impinging on the SiC surface prevents the insertion of the F ions into the network. However, there is no very obvious change of the intensity of C–F groups with the change of etch pressure, as shown in Fig. 8(a). Again, the relative intensity ratio ($I_{\text{semi-ionic}}/I_{\text{covalent}}$) was calculated as described in Sec. III B, as shown in the inset of Fig. 8(b). It illustrates that the lower-F concentration at higher-work pressure and lower-etch rate enhances the relative amount of semi-ionic C–F bonds to covalent bonds.

E. Influence of flow rate

By applying different flow rates of SF_6 and always keeping 20% O_2 accordingly in gas mixtures, SiC samples have also been etched. It is shown in Figs. 9(a) and 9(b) that, although the sample etched at a mixture of 40 sccm SF_6 and 10 sccm O_2 resulted in the relative lowest-dc bias, the highest-etch rate is achieved. Because all these samples were etched at the same pressure (5 mT), the densities of the reactive species in the plasma is the same. However, different flow rates can affect the residence time of the reactive radicals on the being etched SiC surface and also the speed of the removal of the volatile etch products. Higher-flow rate helps to remove the volatile SF_x and CF_x etch products more rapidly. However, when the flow rate is higher than the optimum value, the residence time of the reactive radicals becomes shorter than the time scale inherent to reaction. Therefore, an optimum flow rate is required to achieve better etch rate of SiC.

The relative F concentration is shown in Fig. 9(c). The sample etched at a gas mixture of 40 sccm SF_6 and 10 sccm O_2 has the greatest amount of incorporated F. Although there is no obvious change on the C 1*s* spectra, after the intensity ratio calculation as described in Sec. III B, the lowest $I_{\text{semi-ionic}}/I_{\text{covalent}}$ ratio in the F 1*s* core-level spectra can be

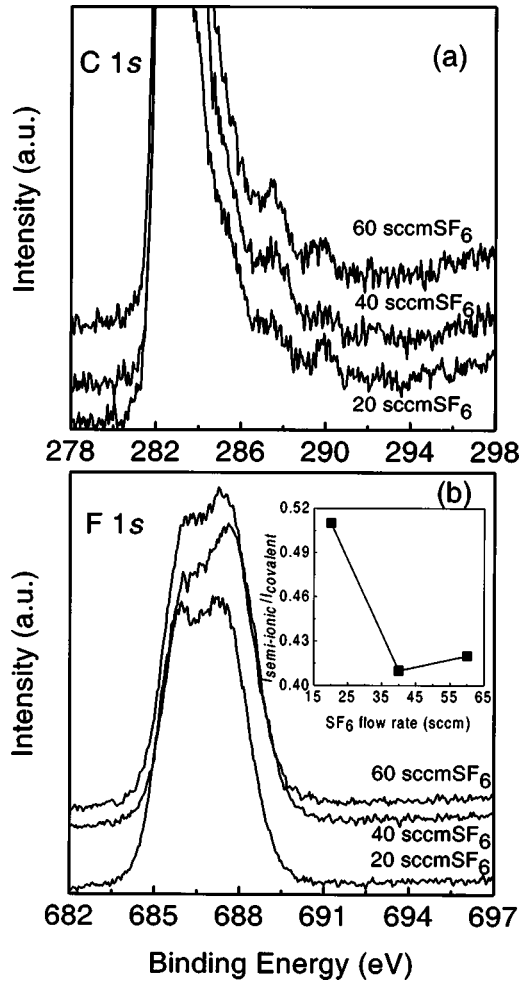

FIG. 10. (a) C 1*s* and (b) F 1*s* photoelectron spectra of SiC surface etched at different SF_6 flow rate. Note that 5, 10, and 15 sccm O_2 were used with 20, 40, and 60 sccm SF_6 in the SF_6/O_2 gas mixtures during etch. (Chuck power = 120 W and pressure = 5 mT).

observed for SiC etched at a gas mixture of 40 sccm SF_6 and 10 sccm O_2, as shown in Fig. 10(b). Again, the etch conditions that produce a higher-etch rate coincides with lower $I_{\text{semi-ionic}}/I_{\text{covalent}}$ ratio, implying that a higher-etch rate can result in a less conductive SiC surface.

IV. CONCLUSIONS

We have etched 4H–SiC in inductively coupled SF_6/O_2 plasma at various etch conditions and both the etch mechanisms and surface chemistry have been systematically investigated. Information of etch-induced surface microstructure modifications have been obtained by XPS measurements. Due to the existence of reactive F ions in the plasma, C–F bonds have been found on etched SiC surfaces. The Si 2*p* spectra of all the etched samples were dominated by Si–C bonds. The absence of Si–Si and Si–F bonds suggests that Si atoms from bond breaking of SiC have been more sufficiently removed than C atoms as volatile etch products.

It is found that in order to achieve a higher-etch rate of SiC, the optimum O_2% in the SF_6/O_2 gas mixture and the flow rate have to be applied during dry etch of SiC. Furthermore, increasing chuck power and decreasing work pressure in the ICP system can also promote the etch processes.

Both C 1*s* and F 1*s* spectra from the etched SiC under various etch conditions have been analyzed and studied. The intensity of the components of C–F groups in the C 1*s* spectra were enhanced with the decrease of O_2% in the gas mixtures. With the increase of the incorporated F content, the formation of C–F bonds follows the order of CF, CF_2, and CF_3. During the studies of F 1*s* spectra, we found that, apart from the results related to the influence of O_2%, in most cases, both the relative F concentration and the $I_{\text{semi-ionic}}/I_{\text{covalent}}$ ratio always follows the similar trend as etch rates. Because covalent C–F bonds exhibit higher resistivity than semi-ionic C–F bonds, this suggests that relative higher-etch rates will result in relatively less conductive SiC etched surfaces. Therefore, as important etch products on the surface of the etched SiC materials, the nature and quantities of the C–F bonds can probably very much affect and explain the behavior of correspondingly fabricated devices such as Schottky diodes.

ACKNOWLEDGMENT

This work was supported by the Engineering and Physical Sciences Research Council (EPSRC) Grant No. GR/R38019/01.

[1] In *Silicon Carbide, A Review of Fundamental Questions and Applications to Current Device Technology*, edited by W. J. Choyke, H. Matsunami, and G. Pensl (Academic, New York, 1997).
[2] K. Xie, J. R. Femish, J. H. Zhao, W. R. Buchwald, and L. Cacas, Appl. Phys. Lett. **67**, 368 (1995).
[3] J. J. Wang, E. S. Lambers, S. J. Pearton, M. Ostling, C. M. Zetterling, J. M. Grow, and F. Ren, Mater. Res. Soc. Symp. Proc. **483**, 177 (1998).
[4] B. Li, L. Cao, and J. H. Zhao, Appl. Phys. Lett. **73**, 653 (1998).
[5] S. W. Pang, in *Surface Damage Induced by Dry Etching, Handbook of Advanced Plasma Processing Technologies*, edited by R. J. Shul and S. J. Pearton (Springer-Verlag, Berlin, 2000).
[6] E. van der Drift, R. Cheung, and T. Zijlstra, Microelectron. Eng. **32**, 241 (1996).
[7] G. McDaniel, J. W. Lee, E. S. Lambers, S. J. Pearton, P. H. Holloway, F. Ren, J. M. Grow, M. Bhaskaran, and R. G. Wilson, J. Vac. Sci. Technol. A **15**, 885 (1997).
[8] M. S. So, S.-G. Lim, and T. N. Jackson, J. Vac. Sci. Technol. B **17**, 885 (1997).
[9] S. M. Kong, H. J. Choi, B. T. Lee, S. Y. Han, and J. L. Lee J. Electron. Mater. **31**, 2009 (2002).
[10] P. Mélnon, P. Kéghélian, A. Perez, C. Ray, J. Lermé, M. Pellarin, M. Broyer, M. Boudeulle, B. Champagnon, and J. L. Rousset, Phys. Rev. B **58**, 16481 (1998).
[11] K. L. Smith and K. M. Black, J. Vac. Sci. Technol. A **2**, 744 (1984).
[12] M. De Seta, N. Tomozeiu, D. Sanvitto, and F. Evangelisti, Surf. Sci. **460**, 203 (2000).
[13] L. Aversa, R. Verucchi, G. Ciullo, L. Ferrari, P. Moras, M. Pedio, A. Pesci, and S. Iannotta, Appl. Surf. Sci. **184**, 350 (2001).
[14] Y. Ma, H. Yang, J. Guo, C. Sathee, A. Agui, and J. Nordgen, Appl. Phys. Lett. **72**, 3353 (1998).
[15] W. K. Choi, T. Y. Ong, L. S. Tan, F. C. Loh, and K. L. Tan, J. Appl. Phys. **83**, 4968 (1998).
[16] Hj. Matzke and J. L. Whitton, Can. J. Phys. **44**, 995 (1966).
[17] H. Naguib and R. Kelly, Radiat. Eff. **25**, 1 (1975).
[18] J. Pezoldt, B. Stottko, G. Kupris, and G. Ecke, Mater. Sci. Eng., B **29**, 94 (1995).
[19] L. Muehlhoff, W. J. Choyke, M. J. Bozach, and J. R. Yates, Jr., J. Appl. Phys. **60**, 2842 (1986).
[20] G. Nansé, E. Papirsr, P. Fioux, F. Moguet, and A. Tressaud, Carbon **35**, 175 (1997).
[21] C. Ronning, M. Büttner, U. Vetter, H. Feldermann, O. Wondratschek, H.

Hofsäss, W. Brunner, F. C. K. Au, Q. Li, and S. T. Lee, J. Appl. Phys. **90**, 4237 (2001).
[22] H. Yang, D. J. Tweet, Y. Ma, and T. Nguyen, Appl. Phys. Lett. **73**, 1514 (1998).
[23] N. Sieber, M. Mollering, and L. Ley, Diamond Relat. Mater. **6**, 1451 (1997).
[24] F. R. McFeely, J. F. Morar, N. D. Shinn, G. Landgren, and F. J. Himpsel, Phys. Rev. B **30**, 764 (1984).
[25] P. H. Yih, V. Saxena, and A. J. Steckl, Phys. Status Solidi B **202**, 605 (1997).
[26] F. A. Khan and I. Adesida, Appl. Phys. Lett. **75**, 2268 (1999).
[27] I. Palchan, M. Crespin, H. Estrade-Szwarckopf, and B. Roussau, Chem. Phys. Lett. **157**, 321 (1989).
[28] A. Tressaud, C. Guimon, V. Gupta, and F. Moguet, Mater. Sci. Eng., B **30**, 61 (1995).
[29] I. Ohana, Phys. Rev. B **39**, 1914 (1989).
[30] W. S. Pan and A. J. Steckl, J. Electrochem. Soc. **137**, 212 (1990).
[31] D. L. Flamm, V. M. Donnelly, and J. A. Mucha, J. Appl. Phys. **52**, 3633 (1981).
[32] D. Briggs and M. P. Seah, in *Practical Surface Analysis* (Wiley, New York, 1983).